

The West African Monsoon Modeling and Evaluation project (WAMME) Initiative and its First Model Intercomparison Experiment: Intercomparison of the WAM climatology

Yongkang Xue¹, K-M Lau², Aaron Boone³, and WAMME team

1). University of California, Los Angeles, CA, USA

2). Goddard Space Flight Center, NASA, MD, USA

3). Centre National de Recherches Météorologiques, Toulouse, France

Abstract

The West African monsoon (WAM) is an important component of the world monsoon system. Understanding the climate of WAM is essential in unraveling the causes of the Sahel drought - the most severe and longest drought in the world during the Twentieth Century. This paper discusses the WAM Modeling and Evaluation project (WAMME) initiative and its approaches to improve WAM simulations. WAMME also investigate interactions of WAM/major external forcing, including sea surface temperature, land surface processes, and aerosols with application of observational and proxy data. This paper evaluates WAMME GCM performances in simulating variability of WAM precipitation, surface temperature, and major circulation features at seasonal and intraseasonal scales in the first WAMME experiment and the role of sea surface temperature, land, are aerosol is also discussed.

Key words: west African monsoon, modeling, SST, land, aerosol

1. Introduction

West Africa (WA) is a diverse climatic region that includes a semi-arid tropical zone in its northern section and a humid tropical climate zone in its southern section. Climate variability in the northern part of WA, the Sahel, shows strong interdecadal signals, and suffered the most severe and longest drought in the world during the Twentieth Century (Redelsperger et al., 2006). Figure 1 shows the Sahel precipitation climatology and its anomalies based on NCEP CPC data. Starting from the late 1980s, however, there has been evidence of some rainfall recovery relative to the very dry period (Figures 1b and 1d). Seasonal and intraseasonal characteristics of WAM rainfall show high interannual variability, which is of prime importance for agricultural development in this populated region (Xue et al., 2004; Baron et al., 2005). The WA climate is strongly affected by external forcings. Among them, sea surface temperature (SST), land surface processes, and aerosols have been identified as major factors. The interannual and interdecadal variability in WA is known to be strongly influenced by SST anomalies, both globally and in regions adjacent to the African continent. Land surface processes have also long been considered a major factor contributing to WAM variability and the drought. Furthermore, North Africa is the world's major source of mineral dust aerosols, which account for about half the global total in recent times. The radiative impact of desert

dust can be expected to be significant in this area due to high dust loading.

2. West African Monsoon Modeling and Evaluation project (WAMME) initiatives for WAM modeling

The WAMME project is a GEWEX/CEOP initiative in collaboration with AMMA, focusing on the use of GCMs and regional climate models (RCMs) to evaluate model ability and uncertainty in simulating major WAM features, associated processes, and their interactions for proper WAM prediction and future climate projections, and to address issues regarding the role of land-ocean-atmosphere interaction, land-use and water-use change, vegetation dynamics, and aerosols, particularly dust, on WAM development. WAMME has conducted its experiment. The first WAMME experiment outputs have been posted on the CEOP database, openly available to the scientific community. Up-to-date WAMME information is posted on the WAMME website: www.wamme.geog.ucla.edu.

In the WAMME project, we plan (1) to evaluate the performance of GCMs and RCMs in simulating WAM precipitation, including WAM onset and withdrawal, and relevant processes at diurnal, intraseasonal, interannual, and interdecadal scales and to identify common discrepancies; (2) to provide better understanding of fundamental physical processes in the WAM; (3) to conduct sensitivity

experiments to isolate important key physical processes for interannual and interdecadal variations of WAM; (4) to demonstrate the utility and synergy of CEOP and AMMA field data in providing a pathway for model physics evaluation and improvement; and (5) to evaluate the nested RCMs' ability to downscale WA regional climate simulations.

3. A combined GCM and RCM approach

WAMME consists of 11 GCMs and 7 RCMs. Among the GCMs, the MRI/JMA GCM has very high horizontal resolution, about 20 km. The NCEP CFS is a coupled ocean/atmosphere model with the NCEP GFS as its atmospheric component. Cornell/NCAR CAM/CLM3.0, GSFC FVGCM, and the University of Cocody RegCM include comprehensive aerosol packages and can be run with or without aerosol. More information on dynamic and physical components of participating models can be found in www.wamme.geog.ucla.edu. Unlike most model comparisons, WAMME includes both GCMs and RCMs.

Figure 2 shows the time evolution of the 5-day mean precipitation average over four years from the first WAMME experiment, in which a 4-member ensemble of model runs simulate the period from April 1, 2, 3, and 4 through October 31 for each of the years 2000, 2003, 2004, and 2005. The RCM simulation shown in Figure 2B has LBC from Reanalysis II. The RCM domain covers 35°W-35°E and 20°S-35°N with about a 0.5 degree horizontal resolution. Also shown in Fig. 2 are the bias and root-mean-squared errors in simulations relative to CPC GTS data, based on six months' simulation and an area average over 0° to 20°N and 10°W to 10°E. Although every model correctly produces the WAM's general evolution, each has substantial deficiencies. For instance, an important feature, the WAM onset jump, is only simulated by some RCMs and MRI/JMA with high horizontal resolution, although the jump is amplified. It may be that coarse GCMs are unable to resolve the heterogeneous spatial-distribution of low level convective instabilities, so that RCMs produce better downscaling for the WAM jump. Despite the variety of deficiencies in individual models, the ensemble means (Figures 2A and 2Bf) produce results in many aspects better than individual model and Reanalyses. Comprehensive discussions of WAMME GCM and RCM performance are presented in Boone et al. (2010), Druyan et al. (2010), and Xue et al (2010).

4 Integrated approach for SST, land, and aerosol forcing

Previous studies have suggested that the complex interactions between the atmosphere,

biosphere, and hydrosphere ultimately determine the nature of the WAM. Thus far, most WA modeling studies are either based on a single model with limited ability to properly simulate every feedback process, or focus on a single external process (such as SST). The integrated investigation of these forcings and feedbacks will be the WAMME approach.

Although the first WAMME experiment is not designed to directly evaluate the influence of specific physical processes, WAMME includes models with different representations of these processes, and comparing the corresponding models' ensemble means allows us to give a preliminary evaluation of the effect of relevant parameterizations/representation and sensitivity of the WAM to these parameterizations/feedbacks to support our combined approach. By comparing results from CFS and GFS, which have the same atmospheric component but predicted SST in CFS and specified SST in GFS, we can assess the impact of interactive SST in the GCM on the WAM simulation. Figure 3a shows that there are substantial differences in four-years mean JJAS precipitation over WA between CFS and GFS, with a zonal dipole pattern. Figure 3b shows the SST difference between these two models. The relationship between the SST anomaly and the Sahel precipitation anomaly shown in Figure 3a and Figure 3b is generally consistent with the SST/Sahel rainfall relationship that has been reported in previous studies.

As for land effects, we examine results from the UCLA GCM, which is coupled with two different land schemes: one is SSiB (Xue et al., 1991) and another one simply prescribing land surface characteristics such as monthly mean surface albedo and ground wetness, which has no land/atmosphere interaction. The differences between the UCLA GCM with these two land schemes show the effect of biophysical processes and land/atmosphere interactions. Figure 3c highlights substantial JJAS precipitation differences between the UCLA GCM runs with two different land surface schemes over WA. There is also a zonal dipole pattern with 10°N as the boundary. Figure 3d shows the latent heat flux difference between these two runs. The UCLA GCM/SSiB produces a larger reduction in evaporation along the Sahel. The relationship between changes in rainfall and evaporation appears in Figures 3c and 3d is consistent with the mechanism reported in previous Sahel land/atmosphere studies (e.g., Xue, 1997).

CAM/CLM3.0 has dust modules in which radiative forcing due to dust is interactive with atmospheric models. Figure 3e shows the JJAS precipitation difference between the run with dust and the run without dust. Only direct effects are included in this experiment. CAM/CLM3.0 shows a rainfall decrease over some areas between 10°N and

15°N and an increase along the coastal area. CAM/CLM3.0 has a wet bias between 15°N and 20°N (Figure 2d), which may be associated with most of the rainfall reduction signal to the north of the Sahel. Figure 3f shows the difference of downward shortwave radiation at the surface. The change in radiative heating affects the low-level moisture convergence and produces rainfall anomalies (Yoshioka et al., 2007; Lau et al., 2008).

In all three cases, changes in external forcing produce a noteworthy dipole, indicating a shifting of the rainfall band. They and aforementioned studies in Section 3 demonstrate the importance of these parameterizations in simulating WAM, and encourage more comprehensive sensitivity studies to integrate all three feedbacks for further investigation.

5. Conclusion

WA has experienced rapid population growth during the past 50 years within a fragile environment. A comparison of different feedback mechanisms, their detail and possible manifestations, uncertainties in their estimation, and interactions between them will provide critical information for the scientific community, the public, and policy-makers. The resultant improved understanding of the causes of WA climate anomalies, will help devise preventative measures against droughts caused by improper human practices, and to develop adaptation strategies. Proper understanding and simulation of the last century's severest and longest drought in the world will also provide a confidence that these models can be used for future WA climate projections.

The WAMME initiative proposes a combined GCM/RCM approach, integrated investigation of major feedback processes and mechanisms, and application of observed and proxy data. The results from the first set of experiments have shown some promise and suggest that our goals can be achieved. WAMME will conduct further experiments to explore the cause of major deficiencies identified in the first WAMME experiment to improve models, and to design specific experiments to evaluate/identify the relative contributions of the three external forcings in WAM variability. Meanwhile, WAMME will continue collaborating with CEOP, AMMA, AMMA-MIP, ALMIP, C20C, EU-ENSEMBLES, and African scientists to achieve the WAMME goals.

Acknowledgement

The WAMME analysis is supported by U.S. NSF grants ATM-0751030 and ATM-0353606

References

Baron C., B. Sultan, M. Balme, B. Sarr, T. Lebel, S. Janicot and M. Dingkuhn, 2005: From GCM grid cell to agricultural plot: scale issues affecting modelling of climate impact. *Phil. Trans. Roy. Soc. B*, 360 (1463), 2095-2108

Boone, A., I. Pocard-Leclercq, Y. Xue, J. Feng, and P. de Rosnay, 2009: Evaluation of the WAMME model surface fluxes using results from the AMMA land-surface model intercomparison project. DOI 10.1007/s00382-009-0653-1.

Druyan, L. M., J. Feng, K. H. Cook, Y. Xue, M. Fulakeza, S. M. Hagos, A. Konare, W. Moufouma-Okia, D. P. Rowell, I. S. Sanda, and E. K. Vizzy, 2009: The WAMME regional model intercomparison study. *Climate Dynamics*. DOI 10.1007/s00382-009-0676-7

Lau, K. M., V. Ramanathan, G.-X. Wu, Z. Li, S. C. Tsay, C. Hsu, R. Sikka, B. Holben, D. Lu, G. Tartari, M. Chin, P. Koudelova, H. Chen, Y. Ma, J. Huang, K. Taniguchi, and R. Zhang, 2008: The joint aerosol-monsoon experiment, a new challenge for monsoon climate research. *Bulletin of the American Meteorological Society*, **89**, 3, 369–383. DOI: 10.1175/BAMS-89-3-369.

Redelsperger, J.-L., C. D. Thorncroft, A. Diedhiou, T. Lebel, D. J. Parker, and J. Polcher, 2006: American monsoon multidisciplinary analysis, *Bull. Amer. Meteor. Soc.*, **88**, 1739-1746.

Xue, Y., P. J. Sellers, J. L. Kinter III, and J. Shukla, 1991: A simplified biosphere model for global climate studies. *J. Climate*, **4**, 345-364.

----, 1997: Biosphere feedback on regional climate in tropical North Africa. *Quart. J. Roy. Met. Soc.*, **123**, B, 1483-1515.

----, Y., F. De Sales, K-M W. Lau, A. Boone, J. Feng, P. Dirmeyer, Z. Guo, K.-M. Kim, A. Kitoh, V. Kumar, I. Pocard-Leclercq, N. Mahowald, W. Moufouma-Okia, P. Pegion, S. D. Schubert, A. Sealy, W. M. Thiaw, A. Vintzileos, M.-L C. Wu, 2009: Intercomparison of West African Monsoon and its Variability in the West African Monsoon Modeling and Evaluation Project (WAMME) First Experiment. *Climate Dynamics*. DOI: 10.1007/s00382-010-0778-2.

Yoshioka, M., N. M. Mahowald, A. J. Conley, W. D. Collins, D. W. Fillmore, C. S. Zender, and D. B. Coleman, 2007: Impact of Desert Dust Radiative Forcing on Sahel Precipitation: Relative importance of dust compared to sea surface temperature variations, vegetation changes and greenhouse gas warming, *J. Climate*, **20**, 1445-1467.

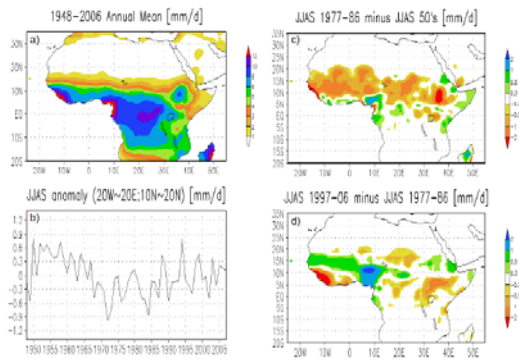


Figure 1. (a) Observed climate annual mean precipitation (mm day⁻¹), (b) Time series of June-July-August-September (JJAS) mean precipitation (mm day⁻¹) averaged over 20°W to 20°E and 5°N to 20°N, (c) Observed JJAS precipitation difference (mm day⁻¹) between the 1980s and the 1950s, (d) Observed JJAS precipitation difference (mm day⁻¹) between 1996-2006 and 1976-1987. Data Source: National Center for Environmental Prediction Climate Prediction Center global land precipitation data.

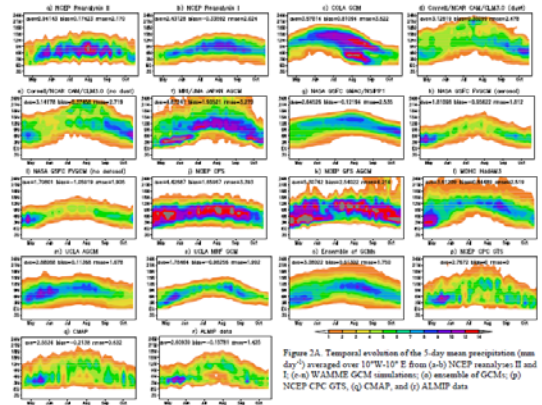


Figure 2A. Temporal evolution of the 5-day mean precipitation (mm day⁻¹) averaged over 10°W-10°E from (a-b) NCEP reanalysis II and II, (c-d) WAMME GCM simulations, (e) ensemble of GCMs, (f) NCEP CPC GTS, (g) CMAP, and (h) ALMIP data.

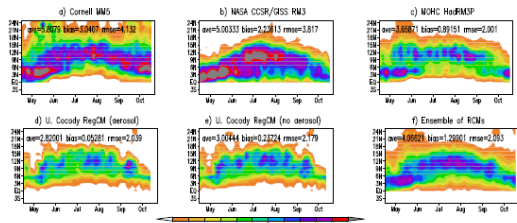


Figure 2B. Temporal evolution of the 5-day mean precipitation (mm day⁻¹) averaged over 10°W-10°E from (a-e) WAMME RCM simulations with NCEP lateral boundary conditions and (f) ensemble of RCMs.

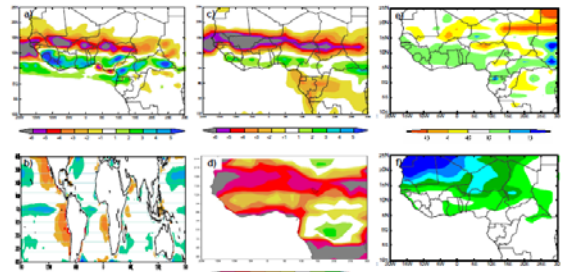


Figure 3. (a) JIAS precipitation difference between NCEP CFS and NCEP GFS (mm day⁻¹), (b) JIAS SST difference between NCEP CFS and NCEP GFS (°C), (c) JIAS precipitation difference between UCLA-SSiB and UCLA-fixed land (mm day⁻¹), (d) JIAS lower heat flux difference between UCLA-SSiB and UCLA-fixed land (mm day⁻¹), (e) JIAS precipitation difference between CAM-CLM3.0 dust and no dust runs (mm day⁻¹), (f) JIAS downward shortwave radiation difference at surface between CAM-CLM3.0 dust and no dust runs (W m⁻²).